Proc. Natl. Acad. Sci. USA
Vol. 94, pp. 849–854, February 1997
Cell Biology

Demonstration of mechanical connections between integrins, cytoskeletal filaments, and nucleoplasm that stabilize nuclear structure

(cell mechanics/cell engineering/tensegrity/extracellular matrix/mechanotransduction)

ANDREW J. MANIOTIS, CHRISTOPHER S. CHEN, AND DONALD E. INGBER

Departments of Pathology and Surgery, Children's Hospital and Harvard Medical School, 300 Longwood Avenue, Boston, MA 02115

Communicated by Robert Langer, Massachusetts Institute of Technology, Cambridge, MA, November 25, 1996 (received for review July 23, 1996)

ABSTRACT **We report here that living cells and nuclei are hard-wired such that a mechanical tug on cell surface receptors can immediately change the organization of molecular assemblies in the cytoplasm and nucleus. When integrins were pulled by micromanipulating bound microbeads or micropipettes, cytoskeletal filaments reoriented, nuclei distorted, and nucleoli redistributed along the axis of the applied tension field. These effects were specific for integrins, independent of cortical membrane distortion, and were mediated by direct linkages between the cytoskeleton and nucleus. Actin microfilaments mediated force transfer to the nucleus at low strain; however, tearing of the actin gel resulted with greater distortion. In contrast, intermediate filaments effectively mediated force transfer to the nucleus under both conditions. These filament systems also acted as molecular guy wires to mechanically stiffen the nucleus and anchor it in place, whereas microtubules acted to hold open the intermediate filament lattice and to stabilize the nucleus against lateral compression. Molecular connections between integrins, cytoskeletal filaments, and nuclear scaffolds may therefore provide a discrete path for mechanical signal transfer through cells as well as a mechanism for producing integrated changes in cell and nuclear structure in response to changes in extracellular matrix adhesivity or mechanics.**

Cells generate mechanical tension in their actin cytoskeleton (CSK) and exert tractional forces on their adhesions to extracellular matrix (ECM) (1). Changes in the balance of forces between cells and ECM, induced by altering matrix flexibility or adhesivity, can change cell shape and switch cells between growth and differentiation (1–5). The precise mechanism by which cell shape changes influence gene expression and cell cycle progression remains unclear. However, these regulatory effects appear to be mediated, at least in part, by associated changes in CSK and nuclear structure (1, 6–10). Thus, it is critical to understand how mechanical stresses applied to the surface membrane can promote coordinated alterations in cell, CSK, and nuclear form. Understanding this mechanism also could provide insight into mechanotransduction, the process by which cells sense and respond to external mechanical stimuli.

One explanation for integrated cell shape control is that transmembrane ECM receptors, CSK filaments, and nuclear scaffolds are "hard-wired" together such that a mechanical pull on the surface membrane results in coordinated realignment of structural elements throughout this interconnected molecular network (11, 12). This model is in direct contrast to many current models of cell mechanics, which envision the viscous fluid-like cytoplasm and surrounding elastic membrane to be the major load-bearing elements in living cells (13–15). On the other hand, microscopic studies demonstrate structural continuity between ECM molecules, transmembrane proteins, CSK filaments, and nuclear scaffolds in detergent-extracted cells (16–18). However, the mechanical relevance of these structural interconnections remains unclear.

We reasoned that if the CSK provides a discrete path for mechanical force transfer from the surface to the nucleus, then we should be able to demonstrate mechanical continuity between cell surface receptors and the nucleus in living cells. To test this hypothesis, we used micropipettes to micromanipulate ligand-coated microbeads (4.5-μm diameter) bound to membrane receptors on cultured endothelial cells. When cells bind to these beads coated with ECM ligands (e.g., fibronectin, RGD-containing peptide) for transmembrane integrin receptors, focal adhesions rapidly form that mediate transfer of mechanical stresses to the internal CSK (12, 19). In contrast, binding of beads coated with acetylated low density lipoprotein (AcLDL), a ligand for transmembrane metabolic receptors, neither promotes focal adhesion formation nor supports efficient stress transfer across the plasma membrane; only a weak connection to the elastic submembranous CSK can be detected (12, 19). In the present study, both types of surface-bound beads were pulled at a rate (approximately 5–10 μm/sec) that was 10 to more than 100 times faster than the fastest assembly rates that have been reported for CSK filaments in mammalian cells (20–22). Using this approach, we now show that cell surface integrin receptors, CSK filaments, and nuclear scaffolds are mechanically coupled in living cells. We also show that the mechanical properties of the cytoplasm and nucleus depend on cooperative force transfer between all three CSK filament systems.

MATERIALS AND METHODS

Experimental System. Bovine capillary endothelial cells were cultured in chemically defined medium on glass coverslips coated with fibronectin at a density (200–400 ng/cm^2; Cappel) that promotes moderate cell spreading; a carbonate buffer coating method was used (2, 7). More highly extended cells are much stiffer (23) and, thus, are less amenable to micromanipulation. Microbeads (4.5 μm, tosyl-activated; Dynal, Oslo) were coated with fibronectin, synthetic RGD peptide (peptide 2000; Telios Pharmaceuticals, San Diego), or AcLDL (Biomedical Technologies, Stoughton, MA) at 50 μg/ml, as described (12, 19), and added to cells (1–4 beads per cell) for 10–15 min at 37°C prior to transfer to an Omega RTD 0.1 stage heating ring coupled to a Nikon Diaphot inverted microscope. An uncoated glass micropipette was placed alongside the surface-bound beads by using a Leitz micromanipulator and then rapidly pulled away from the cell (about 5–10 μm/sec), parallel to dish surface. The micropi-

The publication costs of this article were defrayed in part by page charge payment. This article must therefore be hereby marked "*advertisement*" in accordance with 18 U.S.C. §1734 solely to indicate this fact.

0027-8424/97/94849-6$2.00/0
PNAS is available online at **http://www.pnas.org**.

Abbreviations: CSK, cytoskeleton; ECM, extracellular matrix; AcLDL, acetylated low density lipoprotein; Noc, nocodazole; Acryl, acrylamide; CytoD, cytochalasin D.

pettes were formed with tips approximately 1–5 μm wide along a length of 40–100 μm. In one study, cells with bound beads were permeabilized with 0.5% Triton X-100 in 60 mM Pipes, pH 7.4/25 mM Hepes/8 mM EGTA/2 mM $MgCl_2$ for 2 min at 37°C prior to force application. In other experiments, glass micropipettes were coated directly with integrin ligands (fibronectin or RGD peptide) by using the coating procedure described above. ECM-coated pipettes were held in close contact with the surface of adherent cells for more than 5 min prior to stress application. Control experiments confirmed that cells do not bind to the uncoated glass pipettes in the absence of serum and that surface-bound pipettes could be detached by adding soluble RGD peptide. For polarization microscopy, optics were adjusted to near complete extinction, using a quarter wave plate polarizer in conjunction with Hoya analyzers.

Analysis of Stress Transfer Through the CSK. To identify the molecular basis of force transfer between the CSK and nucleus, we used an uncoated glass micropipette to harpoon the cytoplasm 10 μm from the nuclear border and then pulled away first 10 and then 20 μm at a rate of 5–10 μm/sec. Cells were plated in the absence or presence of 10 μg/ml nocodazole (Noc; Sigma) for 5 hr; 5 mM acrylamide (Acryl; Bio-Rad) for 24 hr; 0.1 μg/ml cytochalasin D (CytoD; Sigma) for 2 hr; or 10 μg/ml Noc for 4 hr followed by 0.1 μg/ml CytoD for 1 hr. These drug doses produce maximal effects on CSK mechanics in these endothelial cells (12). Resultant changes in deformation induced by the 10- and 20-μm pulls were simultaneously measured using real-time videomicroscopy in conjunction with a Macintosh Quadra 800 computer and Oncor Image Analysis software. Nuclear strains in the direction of pull at 10- and 20-μm displacements were calculated as $(d' - d)/d$ and $(d'' - d)/d$, respectively (see Fig. 3*A*). Nuclear movement was defined as displacement of the rear border of the nucleus in the direction of pull (x' and x''). Negative lateral nuclear strain (nuclear narrowing) was calculated by measuring changes in nuclear width perpendicular to the direction of pull.

Analysis of Mechanical Stiffness and Connectivity (Poisson's Ratio) in the Cytoplasm and Nucleus. The stiffness (E) of any material equals stress (σ; force/cross-sectional area) divided by strain (ε; change in length/initial length). Because only induced strains were measured in this study, the stiffness of the cytoplasm and nucleus could not be determined directly. However, we were able to estimate the ratio of stiffnesses in the cytoplasm (c) and nucleus (n) using the following approach. As diagrammed in Fig. 4*A*, the ratio of nuclear to cytoplasmic stiffness (E_n/E_c) will equal the ratio of cytoplasmic to nuclear strain ($\varepsilon_c/\varepsilon_n$) measured in these regions when exposed to the same stress. If the cell responds isotropically and homogeneously to stresses applied over short (micrometer) distances, then the stress tensor (three-dimensional stress field) produced at any point will depend primarily on its location relative to the site of force application. Thus, the ratio of nuclear to cytoplasmic stiffness could be calculated by determining the ratio of induced strains measured in regions of the cytoplasm and nucleus when placed at the same distance from the micropipette.

Strains in the direction of pull were measured within regions of the nucleus and cytoplasm located at the same distance from a pipette that was pulled 10 μm toward the cell periphery; this was accomplished by placing the pipette 5 or 10 μm from the nuclear border (see Fig. 4*A*). When the pipette was placed 10 μm from the nuclear border, induced strains in the direction of pull were measured in the cytoplasm adjacent to the pipette (0–5 μm from the tip), in distal cytoplasm adjacent to the nucleus (5–10 μm away), and in the proximal portion of the nucleus (10–15 μm). Strain was determined, using computerized image analysis, by measuring changes in the distances between different intracytoplasmic or nucleoplasmic phase-dense particles (e.g., vesicles, nucleoli). Identical measurements were then carried out in similarly treated cells with a pipette placed 5 μm from the nuclear border to determine strains at the same distances (0–5, 5–10, or 10–15 μm) from the pipette tip and hence, under similar stresses. These locations now fell in the cytoplasm adjacent to the nucleus, in the proximal nucleus, and in the distal nucleus, respectively (Fig. 4*A*). The ratio of nuclear to cytoskeletal stiffness was calculated by determining the ratio of strains measured in the adjacent cytoplasm and proximal nucleus (i.e., 5–10 μm away from pipettes placed 10 and 5 μm away from the nuclear border, respectively). We also tested our basic assumption by comparing strains measured within adjacent areas in the nucleus (e.g., proximal versus distal) as well as neighboring regions in the cytoplasm (0–5 versus 5–10 μm from the nuclear border), when placed at the same distance from the pipette. Strains measured in these regions did not differ significantly from each other (nucleus/nucleus and cytoplasm/cytoplasm strain ratios ≈ 1), confirming that the stresses were transmitted isotropically and homogeneously, at least over the micrometer distances we analyzed. This approach also assumes that the strength of cell–substrate adhesions and height of the cell in the adjacent 5-μm regions being stressed (n and c) do not vary significantly within similarly treated cells; electron microscopic analysis confirmed that basal adhesions remained relatively constant and that height values differed by only approximately 15%.

Apparent Poisson's ratios were measured in the cytoplasm and nucleoplasm by harpooning cells 10 μm from the nuclear envelope, pulling the pipette 5 μm away from the nuclear border, and calculating the ratio of the strain in the region along the axis perpendicular to the direction of pull divided by the strain in the direction of pull. All strains were measured in equal areas (9 μm^2) equally distant (4–5 μm) from both the pipette and the nuclear border, and all displacements were of equal magnitude. The ratio we report here must be viewed as an "apparent" rather than absolute Poisson's ratio because we calculate the ratio on the basis of a two-dimensional projection of a three-dimensional material in cells adherent to an underlying solid substrate. However, variables were kept constant between measurements and, thus, relative changes in Poisson's ratios may be compared under different experimental conditions.

RESULTS AND DISCUSSION

Mechanical stresses were applied directly to cell surface integrin receptors by allowing cells to bind RGD-coated microbeads (4.5-μm diameter) for 10 min and then pulling these beads laterally, using uncoated glass micropipettes and a micromanipulator. When a single RGD-coated microbead was pulled away from the cell, the nucleus deformed and elongated in the direction of the pull even though it was separated by many micrometers from the site of force application (Fig. 1*A* and *B*). Coordinated changes in intranuclear structure also were produced, as indicated by increases in the spacing between nucleoli (Fig. 1 *A* and *B*). In contrast, when we pulled on AcLDL-beads that bound to transmembrane metabolic receptors that only physically connect to the submembranous CSK [i.e., as opposed to the focal adhesion complex (12, 19)], they detached from the cell surface and no changes in nuclear shape or nucleolar distribution were observed (Fig. 1 *C* and *D*). To determine whether the observed mechanical coupling between integrins and nuclei required changes in diffusion-based chemical signaling or protein polymerization, we pulled integrin-bound beads on cells after membranes and cytosolic components had been extracted with 0.5% Triton X-100 (Fig. 1 *E* and *F*). Again, coordinated distortion of the nucleus and nucleoli was observed, despite the absence of membranes, surface tension, osmotic forces, or ATP, thus confirming that stress can be transferred directly through the CSK lattice.

Living cells were then pulled, using glass micropipettes that were coated directly with integrin ligands to apply stress over larger areas and to rule out potential complications associated with bead internalization. When we pulled fibronectin-coated pipettes that were initially bound to the cell surface many micrometers away from the nucleus, extensive changes in

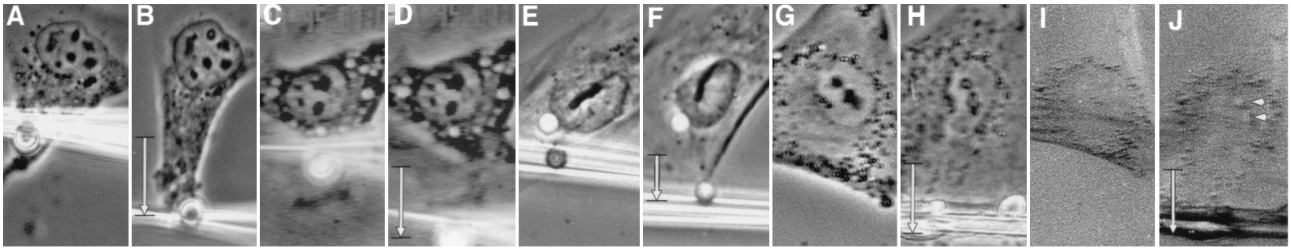

FIG. 1. Phase-contrast (*A–H*) and polarization optics (*I* and *J*) views of endothelial cells before (*A*, *C*, *E*, *G*, and *I*) and after (*B*, *D*, *F*, *H*, and *J*) mechanical stresses were applied to cell surface receptors. (*A* and *B*) Pulling on a single RGD-coated microbead (4.5-μm diameter) 15 min after binding to integrins using an uncoated glass micropipette; only 2 sec passed between *A* and *B*. (*C* and *D*) Similar displacement of a surface-bound AcLDL-coated microbead. (*E* and *F*) Mechanical displacement of RGD-coated beads bound to the surface of a cell permeabilized with 0.5% Triton X-100 prior to force application. (*G* and *H*) A spread cell before (*G*) and after (*H*) a fibronectin-coated micropipette was bound to cell surface integrins for 5 min and pulled laterally (downward in this view). (*I* and *J*) The same cell shown in *G* and *H* viewed under polarization optics; arrowheads indicate white birefringent spots in the region of nucleoli. The movement of the pipette is downward, and vertical black arrows indicate the extent of pipette displacement in all views. (×900.)

nuclear structure were observed, including evagination of the nuclear boundary and elongation of nucleoli along the principal axis of the tension field (Fig. 1 *G* and *H*). Stress-induced molecular reorganization also could be observed within individual nucleoli, as indicated by the appearance of birefringence (i.e., a direct measure of multimolecular realignment) when viewed under polarization optics (Fig. 1 *I* and *J*). In contrast, birefringence of nucleoli was never observed in control cells, regardless of cell or nuclear orientation relative to the direction of the polarizing light. Furthermore, birefringent cytoplasmic filament bundles oriented perpendicular to the pull immediately changed their birefringent sign and, thus, reoriented (i.e., turned 90°) along the major axis of the tension field in response to stress application (Fig. 2 *A* and *B*). These bundles stained positively for F-actin when rhodamine-conjugated phalloidin was used (not shown), and similar realignment of intermediate filaments in response to prolonged pipette pulling has been demonstrated by electron microscopy (24). Nuclear components might be expected to disconnect from integrins in mitotic cells, which lose most of their ECM contacts as well as their nuclear lamina. Nevertheless, when integrins were pulled by using RGD-coated micropipettes, rotation of the mitotic spindle axis and partial separation of chromosomes were observed (Fig. 2 *C–F*).

To analyze the molecular basis of force transfer through the cytoplasm, we used RGD-coated micropipettes to pull on cells that were treated with CytoD and thus lacked intact microfilaments. The surface of these cells distended easily when bound integrins were stressed, at times extending more than 100 μm in length, yet this deformation produced little change in nuclear shape or nucleolar distribution (Fig. 2 *G* and *H*). Thus, deformation of the cortical membrane is not sufficient to produce the nuclear changes that we observed in intact cells.

Because CSK-modifying drugs, such as CytoD, disrupt mechanical signal transfer between integrins and the CSK (12), we used a "harpooning" approach to determine how stress is transmitted from the CSK to the nucleus. The tip of an uncoated micropipette was rapidly inserted into the cytoplasm 10 μm from the outer boundary of the nucleus and pulled first 10 and then 20 μm away toward the cell periphery (Fig. 3*A*). Pulling directly on the CSK resulted in immediate force transfer to the nucleus as indicated by associated nuclear extension (i.e., increase in percent nuclear strain; Fig. 3*B*) and movement of the nucleus in the direction of the pull (Fig. 3*C*) as well as slight narrowing of the nucleus in the perpendicular direction (e.g., $-3.7\% \pm 0.1\%$ lateral strain with 10-μm pipette displacement).

To rule out the possibility that these changes in nuclear shape were produced indirectly by narrowing of the surround-

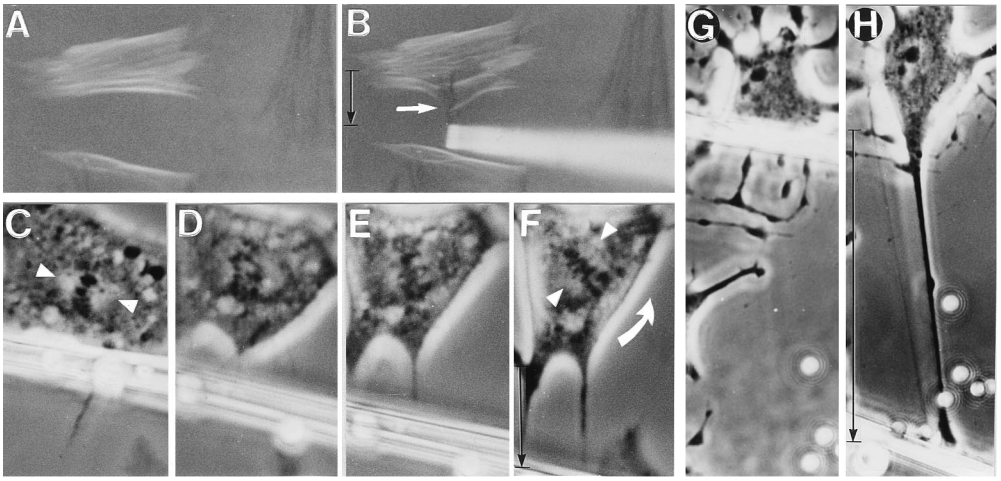

FIG. 2. Polarization optics (*A* and *B*) and phase-contrast (*C–H*) views of interphase (*A*, *B*, *G*, and *H*) and mitotic (*C–F*) cells whose integrin receptors were mechanically stressed by using surface-bound glass micropipettes coated with fibronectin. (*A*) Cells exhibiting positively (white) and negatively (black) birefringent CSK bundles aligned horizontally and vertically, respectively. (*B*) White arrow indicates birefringent CSK bundles that originally appeared white in *A* and immediately changed black as they turned 90° and realigned vertically along the axis of the applied tension field when integrins were pulled. (*C–F*) Series of micrographs showing a living mitotic cell. Pulling on a fibronectin-coated micropipette bound to the cell surface resulted in counterclockwise rotation of the spindle axis. Partial separation of chromosomes also can be seen in *D*. Arrowheads point to the main axis of the spindle in *C* and *F*; curved arrow indicates the direction of spindle rotation. (*G*) An interphase cell treated with 0.1 μg/ml CytoD for 1 hr. (*H*) The same cell as in *G* after tension was applied to integrins by pulling on a surface-bound, matrix-coated micropipette (uncoated 4.5-μm diameter beads were included only for size reference). (*A* and *B*, ×400; *C–G*, ×870; and *G* and *H*, ×520.)

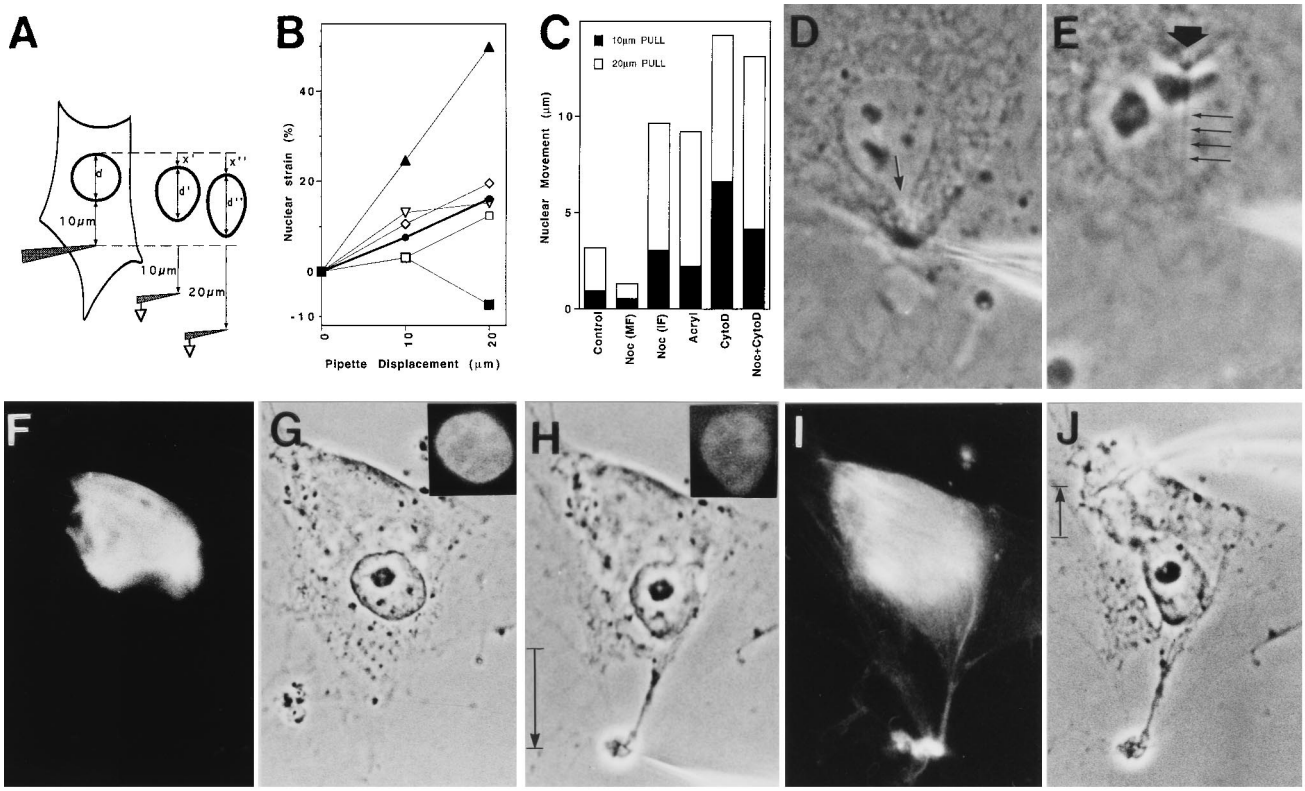

FIG. 3. Analysis of the molecular basis of stress transfer between the CSK and the nucleus. (*A*) Diagram of the method used to determine changes in nuclear strain and movement (see text for details). (*B* and *C*) Effects of CSK-modifying drugs on nuclear strain (*B*) and movement in the direction of pull (*C*); standard error was consistently less than 10% of the mean. ●/Control, absence of drugs; ■/Noc (MF), cells plated in 10 μg/ml Noc for 5 hr and harpooned in the pole of the cell containing only microfilaments; □/Noc (IF), the same Noc-treated cells that were harpooned in the opposite pole containing intermediate filaments; ◇/Acryl, cells treated with 5 mM Acryl for 24 hr; ▲/CytoD, cells treated with 0.1 μg/ml CytoD for 2 hr; ▽/Noc+CytoD, cells in Noc for 4 hr and then in CytoD for 1 hr. (*D*) Control cell harpooned in the cytoplasm 2–4 μm from the nuclear border; arrow indicates a local tongue-like protrusion of the nuclear envelope. (*E*) Invagination of the nuclear envelope (large arrow) in response to harpooning the nucleoplasm. Four small arrows indicate the stressed nucleoplasmic thread stretching to the pipette tip. (*F–J*) Parallel immunofluorescence (*F*, *I*, *Insets* in *G* and *H*) and phase-contrast (*G*, *H*, and *J*) views of a cell that was plated in the presence of Noc, which induced formation of a vimentin-positive intermediate filament cap at one pole of the cell (*F*), although it did not prevent cell or nuclear spreading (*G*). (*H*) Harpooning and pulling the intermediate filament-free pole of the cell caused nuclear elongation in the direction of the pull; however, cytoplasmic tearing also resulted. (*I*) Rhodamine-phalloidin staining of cell depicted in *H*, showing tearing of the F actin-rich pole of the cell that lacked intermediate filaments. (*J*) Cell in *H* after pipette was removed and used to harpoon the cytoplasm on the opposite side of the same cell. Note extensive deformation of the nucleus and narrowing in the perpendicular direction. (*Insets*) Nuclei stained for DNA with 4′,6-diamidino-2-phenylindole (DAPI). (*D*, ×1500; *E*, ×2200; *F–J*, ×1000.)

ing CSK in response to pulling (i.e., a "sausage-casing" effect), we applied tension by means of pipettes placed closer to the nuclear border. If force was transferred to the nucleus indirectly, then tension application would result in global nuclear elongation in the direction of the applied stress, regardless of the site of force application. In contrast, if the CSK transfers stresses to the nucleus across direct mechanical connections, then decreasing the distance between the pipette tip and the nucleus should result in mechanical distortion of progressively smaller regions of the nucleus, with greatest deformation being produced directly along the main axis of the applied tension field. In fact, pulling closer to the nucleus (2–4 μm) caused a small region of the nuclear envelope to protrude locally toward the pipette in the region of highest stress (Fig. 3*D*). Furthermore, the nuclear border and associated cytoplasm also could be made to indent locally by harpooning the nucleoplasm and pulling inward (Fig. 3*E*). A discrete nucleoplasmic thread could be seen stretching from the site of nuclear envelope indentation in these experiments (Fig. 3*E*). These results cannot be explained by a sausage-casing effect and, thus, they confirm that tensional forces are transferred directly from CSK filaments to discrete sites on the nuclear envelope and from there to distinct filamentous networks within the nucleoplasm.

To examine the role of the microfilaments independently of microtubules or intermediate filaments in nuclear shape control, cells were plated in the presence of Noc, which depolymerizes microtubules and induces formation of a contracted intermediate filament cap at one end of the cell (Fig. 3*F*) but permits cell spreading (Fig. 3*G*). The retracted intermediate filament cap can be detected by phase-contrast microscopy as a perinuclear zone of cytoplasm that excludes granules and other organelles. When the opposite side of the cell, which contained only actin filaments, was harpooned, mechanical stress was initially transferred to the nucleus as indicated by localized evagination of the nuclear boundary (Fig. 3*H*) as well as a small increase in nuclear strain (elongation) in the direction of the pull (Fig. 3*B*). But the actin network consistently ruptured in response to larger deformations (Fig. 3 *H* and *I*), causing the stress to dissipate, nuclear movement to cease (Fig. 3*C*), and the extended nucleus to retract (Fig. 3*B*). Importantly, when these cells were pulled from the pole that retained both microfilaments and intermediate filaments, tearing was never observed, and nearly normal nuclear deformation resulted (Fig. 3 *B* and *J*). However, the absence of microtubules resulted in release of the normal restriction to nuclear movement (Fig. 3*C*) as well as a decrease in the ability of the nucleus to resist lateral compression (−13.3% ± 0.7% lateral nuclear strain; Fig. 3*J*). Similar increases in movement (Fig. 3*C*) and lateral compression of the nucleus (−12.8% ± 0.4% strain) were produced when acrylamide was used to disorganize the intermediate filament network in otherwise intact cells, yet nuclear deformation

in the direction of the pull was not altered (Fig. 3*B*). In contrast, disruption of microfilaments with CytoD completely destabilized nuclear shape as well as position, causing the nucleus to become more deformable in both directions (Fig. 3*B*; $-8.1\% \pm 0.4\%$ lateral nuclear strain) and to move freely inside the cell (Fig. 3*C*). Simultaneous administration of CytoD and Noc resulted in additive inhibitory effects on lateral nuclear stability ($-21.5\% \pm 3.4\%$ lateral strain) in addition to destabilizing nuclear position (Fig. 3*C*). Nevertheless, pulling on these cells that lacked both microfilaments and microtubules (i.e., retained only intact intermediate filaments) still produced nuclear deformation and movement in the direction of pull, even at low strains (Fig. 3 *B* and *C*). Thus, the intermediate filament network alone is sufficient to transmit mechanical stress to the nucleus. In round mitotic cells that lack intermediate filaments (Fig. 2), residual actin microfilaments and nuclear matrix scaffolds appear to preserve coupling between the CSK and individual chromosomes (25, 26).

To explore how these CSK interconnections and associated mechanical force transfer contribute to nuclear structure, we measured changes in the relative stiffness of the nucleus compared with the cytoplasm (Fig. 4*A*). This analysis revealed that the nucleus behaved as if it were approximately 9 times stiffer than the cytoplasm in control cells and that this difference in structural rigidity could be completely or partially negated by interfering with microfilaments, intermediate filaments, or microtubules by using appropriate CSK modulators (Fig. 4*B*). Disruption of these filament systems also decreases CSK stiffness (12) and released cytoplasmic restrictions to nuclear movement in these cells (Fig. 3*C*). Thus, given that the nuclear to cytoplasmic stiffness ratio also decreases, treatment with these CSK modulators must result in an even greater loss in nuclear stiffness. Acrylamide could alter nuclear structure directly by compromising the integrity of the nuclear lamina or the intermediate filament cage that surrounds the nucleus (27). CytoD also could have direct effects on internal nuclear scaffolds, since actin has been identified within interphase nuclei (28).

To determine where acrylamide and CytoD exert their destabilizing actions, we compared their effects on the Poisson ratio within the cytoplasm versus nucleoplasm (Fig. 4*B*). Poisson's ratio is a direct mechanical measure of microstructural organization and connectivity within any network (13, 29). We estimated the apparent (two-dimensional) Poisson's ratios by measuring the ratio of the strain perpendicular to the direction of pull divided by the strain in the direction of pull. Treatment of cells with CytoD and acrylamide each independently increased the Poisson ratio in the cytoplasm (Fig. 4*C*), but not in the nucleus (nuclear Poisson's ratios of 0.60 ± 0.10 versus $0.56 + 0.16$, respectively). These drug treatments also did not detectably alter force transfer within the nucleus, as measured using the method shown in Fig. 3*E* (not shown). Acryl and CytoD therefore do not appear to directly influence the structural organization of the nucleoplasm; rather they appear to change the mechanical stability of the nucleus by altering the ability of CSK filaments to act as molecular guy wires within the surrounding cytoplasm.

In solid mechanics, Poisson's ratio typically ranges between 0.3 and 0.5 (30). However, it can reach much higher values in certain solids, such as foams, and particularly in fabrics (29). Our results suggest that the nuclei of living cells also fall into this latter category, as does the cytoplasm after CSK filament disruption. The increase in the cytoplasmic Poisson ratio in response to microfilament disruption may be due to transformation of the CSK from a gel, which typically exhibits a low Poisson ratio, to an open lattice network (due to remaining intermediate filaments and microtubules) that exhibits greater lateral contraction when similarly strained. Acrylamide may increase Poisson's ratio by altering the organization of intermediate filaments or breaking their connections with other filament systems and thereby altering network connectivity. Surprisingly, loss of microtubules induced by Noc resulted in both increased lateral contraction of the cytoplasm (i.e, increased Poisson's ratio; Fig. 4*C*) and enhanced narrowing of the nucleus (increased negative lateral nuclear strain; Fig. 3*J*) in response to tension, even though the gel properties of the actin CSK should become more dominant. Intact microtubules therefore may normally act to stabilize the entire nucleo-CSK lattice against lateral compression, in addition to holding the intermediate filament lattice open in an extended form.

We currently have little understanding of how dynamic and integrated changes in cell form take place or how transmission of mechanical stresses between cells and ECM alters cell and nuclear structure, even though these events clearly play a critical role in growth and differentiation (1–10, 31–32). Our results show that cell surface integrin receptors transmit tensile stresses that mechanically distort interconnected CSK and nucleoskeletal networks and thereby drive changes in cell and nuclear form in time periods much faster than those required for polymerization. While the CSK is surrounded by membranes and penetrated by viscous cytosol, it is this discrete filamentous network that provides the main path for mechanical signal transfer through the cytoplasm. The efficiency of force transfer depends directly on the mechanical properties of the CSK and nucleus, which, in turn, are governed by higher-order cooperative interactions between microfilaments, intermediate filaments, and microtubules acting in the cytoplasm. The CSK also provides the cytoplasm's principal mechanical

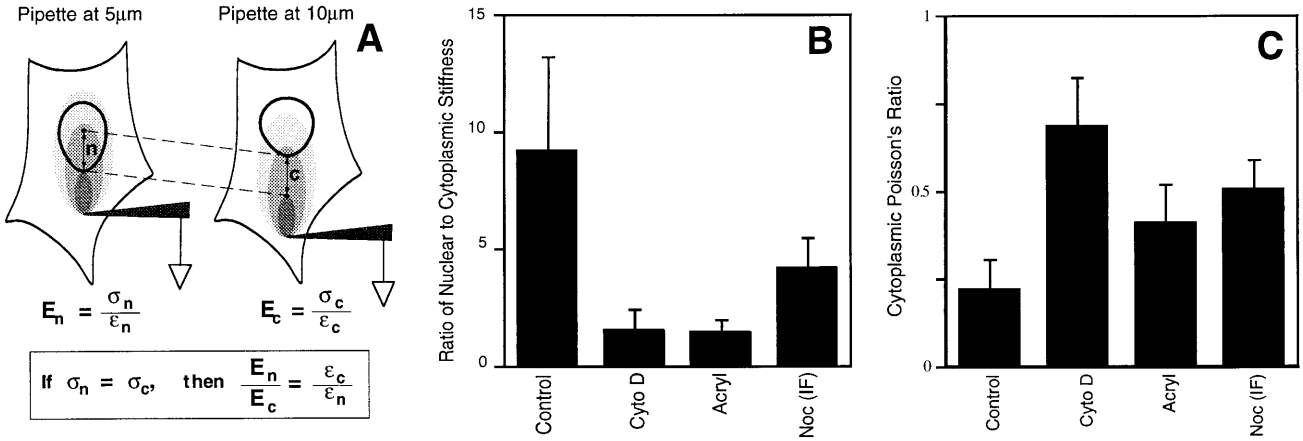

FIG. 4. Analysis of mechanical stiffness and connectivity (Poisson's ratio) in the cytoplasm and nucleus. (*A*) Diagram of the method used to estimate the ratio of nuclear to cytoplasmic stiffness. (*B*) Ratio of nuclear to cytoplasmic stiffness in cells cultured in the absence (Control) or presence of CytoD, Acryl, or Noc (IF), using the conditions described for Fig. 3*C*. (*C*) Poisson's ratio measured in the cytoplasm of control cells (Control) and in cells treated with CytoD, Acryl, or Noc (IF).

strength, whereas the mechanical properties of the surface membrane play a relatively insignificant role in the force balances that determine cell and nuclear form. Importantly, these results not only indicate the inappropriateness of generalizing conventional engineering models of cell mechanics which treat the cell as a viscous fluid surrounded by an elastic membrane or cortical CSK (13–15), they also provide direct evidence in support of more recent efforts to mathematically describe cellular mechanics (33, 34).

Quantitative analysis of the mechanical properties of the cytoplasm and nucleus confirmed that structural interplay in the CSK is complex and that the behaviors of these different filament systems are not simply additive or superimposable. Actin microfilaments form a volume-filling gel that efficiently bears compression, but it does not have the strength to resist external tension and thus, it tears at high strain. The intermediate filament network is itself poor at resisting lateral compression, yet it efficiently resists tension and hardens at high strains. Similar results have been obtained by studying purified filament systems *in vitro* (35). However, when these two filament systems are combined in living cells, a composite higher-order structure is formed that provides both load-bearing functions with greater efficiency. Full mechanical responsiveness and structural stability, however, require the added presence of microtubules to locally resist the inward contraction of the surrounding tensile CSK and thereby, to impose an internal stress or "prestress" in this interconnected molecular network. Cytoplasmic microfilaments and intermediate filaments also appear to act as tensile guy wires that anchor the nucleus in place, coordinate changes in cell and nuclear form, and provide the nucleus with its own mechanical stiffness.

This observed dependence on discrete load-bearing elements, tensional continuity, and prestress for shape stability is consistent with a model of cell and tissue structure that is based on tensegrity architecture (11). Tensegrity can explain how local stresses produce coordinated changes in cell, CSK, and nuclear structure in the absence of protein polymerization or diffusion-based signaling (ref. 12; Fig. 1) and how different types of CSK filaments can contribute uniquely to the overall mechanical behavior of the cell. It also provides a mathematical basis to predict the material properties and architectural features of living cells, independent of changes in CSK connections (11, 33). This is in contrast to percolation theory, which is a mathematical method for analyzing the importance of phase transitions and connectivity within networks (34). While tensegrity provides a mathematical basis for shape stability (33), percolation provides a complementary approach to describe how the mechanical behavior of tensegrity-based networks may change in response to alterations in CSK polymerization or cross-linking.

Taken together, these results indicate that cells and nuclei are literally built to respond directly to mechanical stresses applied to cell surface receptors, such as integrins. Other types of adhesion receptors that couple to the CSK (e.g., cadherins) may exhibit similar behavior. The demonstration of direct mechanical linkages throughout living cells raises the possibility that regulatory information, in the form of mechanical stresses or vibrations, may be rapidly transferred from these cell surface receptors to distinct structures in the cell and nucleus, including ion channels, nuclear pores, nucleoli, chromosomes, and perhaps even individual genes, independent of ongoing chemical signaling mechanisms. As an example, neurotransmitter release from motor nerve terminals can be detected within 10–20 msec after cell surface integrins are mechanically stressed (36). Direct mechanical stress transfer across these CSK linkages also may explain the coupling between cell and nuclear shape that is observed in spreading (6, 9) and retracting cells (37); why nuclear pores expand and nuclear transport rates increase when cells physically extend (38); and how changes in the distribution of mechanical stresses transmitted across integrins might redirect the axis of cell division, a process that is critical for morphogenesis of plants (39) as well as animals. This type of "mechanical signaling" (i.e., structural coupling) could serve to coordinate, complement, and constrain slower diffusion-based chemical signaling pathways (1, 11) and, thus, explain in part how mechanical distortion of ECM caused by gravity, hemodynamic forces, or cell tension can change cell shape, alter nuclear functions, and switch cells between different genetic programs.

We thank T. N. Chen, R. Ezzell, T. Pedersen, N. Wang, K. Mi-Lee, J. Fong, and M. Chicurel for helpful suggestions and J. Folkman and R. Cotran for their continued support. This work was supported by grants from the National Institutes of Health (CA-45548) and the National Aeronautics and Space Administration (NAG-9-430).

1. Ingber, D. E. (1991) *Curr. Opin. Cell Biol.* **3,** 841–848.
2. Ingber, D. E. & Folkman, J. (1989) *J. Cell Biol.* **109,** 317–330.
3. Singhvi, R., Kumar, A., Lopez, G., Stephanopoulos, G. N., Wang, D. I. C. & Whitesides, G. M. (1994) *Science* **264,** 696–698.
4. Maniotis, A. J. & Schliwa, M. (1991) *Cell* **67,** 495–504.
5. Li, M. L., Ageller, J., Farson, D. A., Hatier, C., Hassell, J. & Bissell, M. J. (1987) *Proc. Natl. Acad. Sci. USA* **84,** 136–140.
6. Ingber, D. E., Madri, J. A. & Folkman, J. (1987) *In Vitro Cell Dev. Biol.* **23,** 387–394.
7. Ingber, D. E., Prusty, D, Sun, Z, Betensky, H. & Wang, N. (1995) *J. Biomech.* **28,** 1471–1484.
8. Bohmer, R.-M., Scharf, E. & Assoian, R. K. (1996) *Mol. Biol. Cell* **7,** 101–111.
9. Pienta, K. J. & Coffey, D. S. (1992) *J. Cell. Biochem.* **49,** 357–365.
10. Yen, A. & Pardee, A. B. (1978) *Science* **204,** 1315–1317.
11. Ingber, D. E. (1993) *J. Cell Sci.* **104,** 613–627.
12. Wang, N., Butler, J. P. & Ingber, D. E. (1993) *Science* **260,** 1124–1127.
13. Fung, Y. C. (1988) *Biomechanics: Mechanical Properties of Living Tissues* (Springer, New York).
14. Evans, E. & Yeung, A. (1989) *Biophys. J.* **56,** 151–160.
15. Lauffenburger, D. A. & Linderman, J. J. (1993) *Receptors: Models for Binding, Trafficking, and Signaling* (Oxford Univ. Press, New York).
16. Berezney, R. & Coffey, D. S. (1975) *Science* **189,** 291–293.
17. Fey, E. G., Wan, K. M. & Penman, S. (1984) *J. Cell Biol.* **98,** 1973–1984.
18. Osborn, M. & Weber, K. (1977) *Exp. Cell Res.* **106,** 339–349.
19. Plopper, G. & Ingber, D. E. (1993) *Biochem. Biophys. Res. Commun.* **193,** 571–578.
20. Condeelis, J. (1993) *Annu. Rev. Cell Biol.* **9,** 411–444.
21. Gelfand, V. I. & Bershadsky, A. D. (1991) *Annu. Rev. Cell Biol.* **7,** 93–116.
22. Fuchs, E. & Weber, K. (1994) *Annu. Rev. Biochem.* **63,** 345–382.
23. Wang, N. & Ingber, D. E. (1994) *Biophys. J.* **66,** 2181–2189.
24. Kolega, J. (1986) *J. Cell Biol.* **102,** 1400–1411.
25. Maniotis, A., Bojanowski, K. & Ingber, D. E. (1997) *J. Cell. Biochem.*, in press.
26. Nickerson, J., Krockmalnic, K., Wan, M. & Penman, S. (1992) *J. Cell Biol.* **116,** 977–987.
27. Hay, M. & De Boni, U. (1991) *Cell Motil. Cytoskeleton* **18,** 63–68.
28. Amankwah, K. S. & De Boni, U. (1994) *Exp. Cell Res.* **210,** 315–325.
29. Gibson, L. J. & Ashby, M. F. (1988) *Cellular Solids: Structure and Properties* (Pergamon, New York).
30. Crandall, S. H, Dahl, N. C. & Lardner, T. J. (1978) *An Introduction to the Mechanics of Solids* (McGraw–Hill, New York).
31. Folkman, J. & Moscona, A. (1978) *Nature (London)* **273,** 345–349.
32. Ingber, D. E., Madri, J. A. & Jamieson, J. D. (1986) *Am. J. Pathol.* **122,** 129–139.
33. Stamenovic, D., Fredberg, J., Wang, N., Butler, J. & Ingber, D. (1996) *J. Theor. Biol.* **181,** 125–136.
34. Forgacs, G. (1995) *J. Cell Sci.* **108,** 2131–2143.
35. Janmey, P. A., Euteneur, U., Traub, P. & Schliwa, M. (1991) *J. Cell Biol.* **113,** 155–161.
36. Chen, B. M. & Grinnell, A. D. (1995) *Science* **269,** 1578–1580.
37. Sims, J. R., Karp, S. & Ingber, D. E. (1992) *J. Cell Sci.* **103,** 1215–1222.
38. Feldherr, C. M. & Akin, D. (1990) *J. Cell Biol.* **111,** 1–8.
39. Lintilhac, P. M. & Vesecky, T. B. (1984) *Nature (London)* **307,** 363–364.